Journal of
Mechanics of
Materials and Structures

DISPLACEMENT CAPACITY OF MASONRY STRUCTURES UNDER HORIZONTAL ACTIONS VIA PRD METHOD

Antonino Iannuzzo, Carlo Olivieri and Antonio Fortunato

Volume 14, No. 5 December 2019

msp

JOURNAL OF MECHANICS OF MATERIALS AND STRUCTURES
Vol. 14, No. 5, 2019
dx.doi.org/10.2140/jomms.2019.14.703

DISPLACEMENT CAPACITY OF MASONRY STRUCTURES UNDER HORIZONTAL ACTIONS VIA PRD METHOD

ANTONINO IANNUZZO, CARLO OLIVIERI AND ANTONIO FORTUNATO

The displacement capacity of masonry structures, investigated through the piecewise rigid displacement (PRD) method, is the principal focus of the present study. Since a masonry construction exhibits a rigid block mechanism when shaken by severe earthquakes, by adopting the Heyman material restrictions, the PRD method can be used to look for the global collapse mechanism of the structure under horizontal actions and the static load multiplier. As a result of this investigation, a one-degree of freedom mechanism is detected. In the moving part of the collapsing structure, the field of relative displacement among the blocks allows to identify the fracture distribution. The paper examines the stability of masonry constructions analysing the displacement capacity curves which is obtained by a kinematical incremental analysis via PRD method, operating in the framework of limit analysis. The displacement capacity of the structure is defined as the maximum displacement in which the potential energy assumes a local maximum. Consequently, the moving part of the structure in this configuration is unstable. Finally, two examples are exposed in detail to show the performance of the PRD method.

1. Introduction

In many technical regulations, it is requested to assess the displacement capacity of masonry structures under seismic loads. This represents one of the recent and current critical issues (see [Ochsendorf 2006]) in the analysis of unreinforced masonry structures, and many numerical codes, with more or less success, were recently developed in order to answer to this request. Most of them are implemented in Finite Element (FE) environment and take into account geometric and mechanical nonlinearities, but, in most of the cases, without considering unilateral contacts between elements. Although there is a possibility to use FE codes implementing a finite number of unilateral contacts the results are often not satisfactory as shown in [Shin et al. 2016]. The phenomenological behaviour involving the unilaterality of masonry structures is better taken in account by discrete element methods (DEM) [Cundall 1971] with commercial software such as 3DEC (see [Drei et al. 2016; Forgács et al. 2017; Simon and Bagi 2016; Sarhosis et al. 2016; Tóth et al. 2009]). DEM codes model the unilateral contact among blocks by considering special friction laws at interfaces. The solutions obtained depend crucially on the initial configuration and on the load history. Our aim is to explore the stability of masonry structures and then to evaluate their displacement capacity curves in the framework of limit analysis by using the piecewise rigid displacement (PRD) method. Heyman [1966] fixed in a rigorous and a clear way the theoretical basis for the application of limit analysis to generic masonry structures through the formulation of three simple basic

Ianuzzo is the corresponding author.
Keywords: masonry, unilateral materials, stability, piecewise rigid displacements, concentrated cracks, displacement capacity.

material restrictions: (i) masonry has no tensile strength, (ii) masonry has infinite compressive strength, (iii) sliding does not occur.

These three hypotheses represent sufficient assumptions for the application of the two basic theorems of limit analysis to masonry structures. For the discussion and the application of limit analysis to masonry-like structures the reader can examine the works in [Livesley 1978; Como 1992; Angelillo 2014; 2015; 2019; Block 2009; Huerta 2008; Sacco 2014; Brandonisio et al. 2013; 2015; 2017; Cennamo and Di Fiore 2013; Cennamo et al. 2018; Chiozzi et al. 2017; Gesualdo et al. 2017; Angelillo et al. 2014; 2018; Block et al. 2006b; Block and Lachauer 2013; Fortunato et al. 2015; 2018; Fraddosio et al. 2019; Iannuzzo et al. 2018c; Portioli et al. 2014].

On adopting for the material Heyman's restrictions, the stability of some masonry structures under finite displacement is implemented parametrically by solving the equilibrium problem via thrust line in [Block et al. 2006a; Zampieri et al. 2018]. On the other hand, the displacement capacity can be explored dynamically by using DEM as in [McInerney and DeJong 2015] or comparing DEM results with laboratory tests (see [Rossi et al. 2017; Misseri et al. 2018; Van Mele et al. 2012]). Portioli and Cascini [2016] assess the stability of some simple structures by using rigid block limit analysis.

2. Material restrictions, BVP and the energy criterion for NRNT materials

NRNT materials. Heyman's constraints (i), (ii), (iii) can be extended to 2D continua on introducing unilateral material restrictions on the stress and on strain. A 2D masonry structure is modelled as a continuum occupying the region Ω of the Euclidean space $\mathscr{E}^2$. Within the small displacement assumption, we denote $\boldsymbol{T}$ the stress inside Ω, $\boldsymbol{u}$ the displacement of material points $\boldsymbol{x}$ belonging to Ω and adopt the infinitesimal strain $\boldsymbol{E}$ as the strain measure.

A normal rigid no-tension (NRNT) material is one that satisfies the following restrictions:

$$\boldsymbol{T} \in \mathrm{Sym}^-, \quad \boldsymbol{E} \in \mathrm{Sym}^+, \quad \boldsymbol{T} \cdot \boldsymbol{E} = 0, \tag{1}$$

where Sym^-, Sym^+ are the mutually polar cones of negative and positive semidefinite symmetric tensors. The restrictions (1) are equivalent to the so-called normality conditions

$$\boldsymbol{T} \in \mathrm{Sym}^-, \quad (\boldsymbol{T} - \boldsymbol{T}^*) \cdot \boldsymbol{E} \geq 0, \quad \forall \boldsymbol{T}^* \in \mathrm{Sym}^-, \tag{2}$$

and to the *dual normality conditions*:

$$\boldsymbol{E} \in \mathrm{Sym}^+, \quad (\boldsymbol{E} - \boldsymbol{E}^*) \cdot \boldsymbol{T} \geq 0, \quad \forall \boldsymbol{E}^* \in \mathrm{Sym}^+. \tag{3}$$

The restrictions defining an NRNT material in the particular form (2) are the essential ingredients for the application of the theorems of limit analysis (see [Kooharian 1952; Giaquinta and Giusti 1985; Fortunato et al. 2014; 2016]).

The boundary value problem. The equilibrium of a 2D masonry structure, modelled as a continuum made of an NRNT material subject to given loads and settlements, can be formulated as a boundary value problem (BVP), in the following form: "*Find a displacement field* $\boldsymbol{u}$ *and the allied strain* $\boldsymbol{E}$*, and a* *stress field $\boldsymbol{T}$ such that*

$$\boldsymbol{E} = \tfrac{1}{2}(\nabla \boldsymbol{u} + \nabla \boldsymbol{u}^T), \quad \boldsymbol{E} \in \mathrm{Sym}^+, \quad \boldsymbol{u} = \bar{\boldsymbol{u}} \text{ on } \partial\Omega_{\mathrm{D}}, \tag{4}$$

$$\mathrm{div}\boldsymbol{T} + \boldsymbol{b} = 0, \quad \boldsymbol{T} \in \mathrm{Sym}^-, \quad \boldsymbol{T}\boldsymbol{n} = \bar{\boldsymbol{s}} \text{ on } \partial\Omega_{\mathrm{N}}, \tag{5}$$

$$\boldsymbol{T} \cdot \boldsymbol{E} = 0,\text{"} \tag{6}$$

where $\boldsymbol{n}$ is the unit outward normal to the boundary $\partial\Omega$, and $\partial\Omega_{\mathrm{D}}$, $\partial\Omega_{\mathrm{N}}$ is a fixed partition of the boundary into constrained and loaded parts [Angelillo and Fortunato 2004].

Concentrated strain and stress. For NRNT materials, it's well known that the strain and stress are bounded measures and can be decomposed into the sum of two parts

$$\boldsymbol{E} = \boldsymbol{E}^r + \boldsymbol{E}^s, \quad \boldsymbol{T} = \boldsymbol{T}^r + \boldsymbol{T}^s, \tag{7}$$

where $(.)^r$ is the regular part (i.e., the part which is absolutely continuous with respect to the area measure) and $(.)^s$ is the singular part.

A nonzero singular part of the strain or also of the stress substantiates the possibility of admitting discontinuities of the displacement vector and of the stress vector across certain curves. For a more detailed review about jump discontinuities of stress or of displacement the reader could look at [Angelillo and Rosso 1995; Angelillo et al. 2005; 2010; 2012; 2016].

Displacement approach. With respect to a given structure under given loads and distortions, a solution of the BVP through the *displacement approach* consists in the search of a displacement field $\boldsymbol{u} \in \mathcal{K}$ for which there exist a stress field $\boldsymbol{T} \in \mathcal{H}$ such that $\boldsymbol{T} \cdot \boldsymbol{E}(\boldsymbol{u}) = 0$, where $\mathcal{K}$ and $\mathcal{H}$ are the sets of kinematically admissible displacements and stresses, defined by

$$\mathcal{K} = \{\boldsymbol{u} \in S / \boldsymbol{E} = \tfrac{1}{2}(\nabla \boldsymbol{u} + \nabla \boldsymbol{u}^T) \in \mathrm{Sym}^+ \quad \text{and} \quad \boldsymbol{u} = \bar{\boldsymbol{u}} \text{ on } \partial\Omega_{\mathrm{D}}\}, \tag{8}$$

$$\mathcal{H} = \{\boldsymbol{T} \in S' / \mathrm{div}\boldsymbol{T} + \boldsymbol{b} = 0, \quad \boldsymbol{T} \in \mathrm{Sym}^-, \quad \boldsymbol{T}\boldsymbol{n} = \bar{\boldsymbol{s}} \text{ on } \partial\Omega_{\mathrm{N}}\}, \tag{9}$$

where S, S' are two suitable function spaces.

Energy criterion. The energy $\mathcal{P}(\boldsymbol{u})$ for Heyman's materials is just the potential energy of the loads [De Serio et al. 2018], namely

$$\mathcal{P}(\boldsymbol{u}) = -\int_{\partial\Omega_{\mathrm{N}}} \bar{\boldsymbol{s}} \cdot \boldsymbol{u} \, \mathrm{d}s - \int_{\Omega} \boldsymbol{b} \cdot \boldsymbol{u} \, \mathrm{d}a. \tag{10}$$

The search of a solution of the BVP through a displacement approach could be performed by looking for the minimizer $\boldsymbol{u}^0$ of $\mathcal{P}(\boldsymbol{u})$:

$$\mathcal{P}(\boldsymbol{u}^0) = \min_{\boldsymbol{u} \in \mathcal{K}} \mathcal{P}(\boldsymbol{u}) \quad \text{with } \boldsymbol{u} \in \mathcal{K}. \tag{11}$$

The search of an approximate solution: PRD Method. The idea at the base of the PRD Method is to approximate the solution of the BVP by restricting the search of the minimizer to a proper subset of $\mathcal{K}$, that is by minimizing the energy function in the set $\mathcal{K}_{\mathrm{pr}} \subset \mathcal{K}$ of piecewise rigid displacements (PRD) verifying Heyman's material restrictions, that is

$$\mathcal{K}_{\mathrm{pr}} = \{\boldsymbol{u} \in \mathcal{S}_{\mathrm{PR}} / \boldsymbol{E} \in \mathrm{Sym}^+ \quad \text{and} \quad \boldsymbol{u} = \bar{\boldsymbol{u}} \text{ on } \partial\Omega_{\mathrm{D}}\} \subset \mathcal{K}, \tag{12}$$

where $\mathcal{K}_{\mathrm{pr}}$ is an infinite dimensional space and can be discretized by fixing a proper finite subset, called $\mathcal{K}_{\mathrm{pr}}^M$, generated by a finite polygonal partition of the structural domain Ω into rigid parts Ω_i, say

$$(\Omega_i)_{i\in\{1,2,\dots,M\}}. \tag{13}$$

The minimizer $\boldsymbol{u}_{\mathrm{PR}}^0 \in \mathcal{K}_{\mathrm{pr}}^M$ of the potential energy, namely

$$\mathcal{P}(\boldsymbol{u}_{\mathrm{PR}}^0) = \min_{\boldsymbol{u}\in\mathcal{K}_{\mathrm{pr}}^M} \mathcal{P}(\boldsymbol{u}), \tag{14}$$

represents an approximation of the solution $\boldsymbol{u}^0$ of the exact problem (11) in the subset $\mathcal{K}_{\mathrm{pr}}^M$ and, in this sense, represents the solution of the BVP by using the PRD Method. The way used to numerically implement the problem (14) is treated in deep in other papers, e.g., [Angelillo et al. 2018; Iannuzzo 2017; 2018c; 2018b]. For completeness, here the main steps needed to numerically implement problem (14) in order to transform it in a typical linear programming problem are reported. $\mathcal{K}_{\mathrm{pr}}$ is assumed as the discretized kinematical admissible displacements set generated by the partition of the domain Ω into M rigid polygons Ω_i, whose boundary $\partial\Omega_i$ is the union of straight *interfaces* $\partial\Omega_i^j$ with unit normal $\boldsymbol{n}_{ij}$ and tangent vector $\boldsymbol{t}_{ij}$. By restricting to PRD displacements, the strain $\boldsymbol{E}$ coincides with its singular part $\boldsymbol{E}^s$ and can be written with reference to the partition (13) as

$$\boldsymbol{E} = \boldsymbol{E}^s = \sum_{ij} v_{ij}\,\delta(\partial\Omega_i^j)\,\boldsymbol{u}_{ij}\otimes\boldsymbol{n}_{ij} + \frac{1}{2}\sum_{ij} w_{ij}\,\delta(\partial\Omega_i^j)(\boldsymbol{t}_{ij}\otimes\boldsymbol{n}_{ij}+\boldsymbol{n}_{ij}\otimes\boldsymbol{t}_{ij}), \tag{15}$$

where $\delta(\partial\Omega_i^j)$ is the unit line Dirac delta with support on the interfaces $\partial\Omega_i^j$ belonging to the skeleton of the mesh. The Heyman's restrictions are taken into account by enforcing the normality conditions (2) on the strain, that is by writing, for each interface $\partial\Omega_i$, the two following conditions:

$$v_{ij} = [\boldsymbol{u}]\cdot\boldsymbol{n}_{ij} \geq 0, \tag{16}$$

$$w_{ij} = [\boldsymbol{u}]\cdot\boldsymbol{t}_{ij} = 0, \tag{17}$$

where $[\boldsymbol{u}]$ denotes the displacement jump associated to the generic piecewise rigid displacement $\boldsymbol{u} \in \mathcal{K}_{\mathrm{pr}}^M$. It is worth to note that conditions [(16), (17)] enforce unilateral contact with no sliding on the interface $\partial\Omega_i$. Since $\boldsymbol{u} \in \mathcal{K}_{\mathrm{pr}}^M$ is in one to one correspondence with a vector $\boldsymbol{U} \in \mathbb{R}^{3M}$ whose components represent the $3M$ degree of freedom of the element Ω_i, both the energy function $\mathcal{P}(\boldsymbol{u})$ and the restrictions [(16), (17)] can be expressed in terms of $\boldsymbol{U}$; in particular relations [(16), (17)] , written at each interface, can be transformed into matrix forms:

$$\boldsymbol{A}\boldsymbol{U} \geq \boldsymbol{0}, \tag{18}$$

$$\boldsymbol{B}\boldsymbol{U} = \boldsymbol{0}. \tag{19}$$

Finally, the minimum problem (14) which approximates the minimum problem (11) can be transformed into

$$\mathcal{P}(\boldsymbol{U}^0) = \min_{\widehat{\boldsymbol{U}}\in\mathbb{K}^M} \mathcal{P}(\boldsymbol{U}), \tag{20}$$

where $\mathbb{K}^M$ is the set

$$\mathbb{K}^M = \{\boldsymbol{U} \in \mathbb{R}^{3M} / \boldsymbol{A}\boldsymbol{U} \geq \boldsymbol{0}, \quad \boldsymbol{B}\boldsymbol{U} = \boldsymbol{0}\}. \tag{21}$$

Problem (20) is a standard linear finite dimensional minimization problem, since the function $\mathcal{P}(\widehat{\boldsymbol{U}})$ is a linear functional of the 3M-vector $\widehat{\boldsymbol{U}}$ and all the constraints are represented by linear conditions. Furthermore, it is worth to note that problem (20) transforms the original minimization problem (11) for a continuum, into a minimization problem for a multibody structure subject to unilateral contact conditions along the interfaces. The solution can be searched with the simplex method [Dantzig et al. 1955] or, if the number of variables is large, one can resort to the interior point algorithm (see [Mehrotra 1992; Vanderbei 2015; Dantzig 1963]).

Seismic analysis. The object of the present study is to assess the bearing capacity of masonry structures under seismic actions. Horizontal seismic actions, modelled as static, are gradually increased by considering forces proportional to the mass through the scalar parameter λ (for reference see [Iannuzzo 2017; Iannuzzo et al. 2018b]).

In order to solve this problem and to evaluate the horizontal collapse multiplier λ_c, with our approach, we proceed as follows. Denoting λ the scale factor of the horizontal actions we can find an interval $[\lambda_s, \lambda_m]$ to which the collapse multiplier λ_c has to belong. In particular, λ_s represents an approximation of the supremum of the multipliers for which the initial configuration is still safe (i.e., $\widehat{\boldsymbol{U}}^0 = \mathbf{0}$) whilst λ_m represents an approximation of the infimum of the multipliers for which the structure becomes a mechanism (i.e., $\widehat{\boldsymbol{U}}^0 \to \infty$).

3. Capacity curves with PRD method: two examples

In this section two trivial examples concerning the evaluation of the static displacement capacity of two masonry structures are reported: the first one concerns a circular arch whilst the second refers to a simple portal.

First, via the PRD method (see [Iannuzzo et al. 2018a]), the horizontal static multiplier λ_m and the relative one-degree of freedom mechanism is detected. Then, beginning from this last mechanism, an incremental kinematic procedure is undertaken. In particular, the mechanism corresponding to λ_m is used to start a step-by-step kinematical procedure in order to assess the maximum horizontal displacement. To preserve linearity, the macroblocks are considered rigid and the incremental kinematical analysis is conducted by considering the superposition of small rigid displacements: the geometry of the structure at the generic step is obtained by upgrading, in an incremental step-by-step process, the previous configuration. In this incremental analysis, the governing Lagrangian parameter increases with fixed value δq at each step j, so that the evolution of the configuration of the structure depends on the step j. At the same time, by evaluating the infinitesimal incremental work made by the external gravitational forces, a curve describing the upgraded total potential energy is obtained. The displacement capacity of the structure is assumed as the displacement for which the total potential energy admits a local maximum with respect to λ. Such a state represents an unstable equilibrium configuration. Moreover, this approach can allow to extend rocking analyses (see [Gesualdo et al. 2018]) to masonry structures.

Two numerical analyses, presented below, are developed in Mathematica [Wolfram 2003] through a numerical procedure based on the following main steps:

(1) definition of the structural geometry and its discretization;

(2) representation of the piecewise rigid displacement field over the given support (discretized partition);

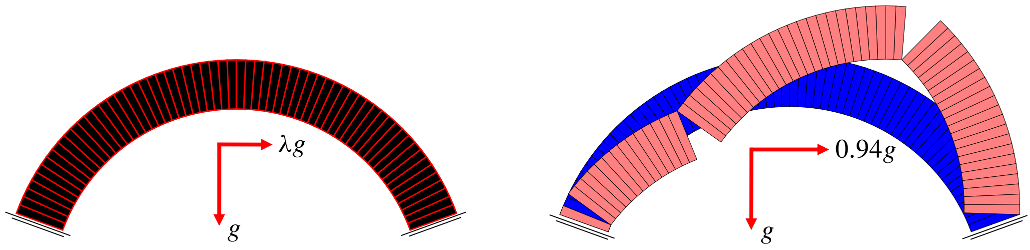

Figure 1. Left: the circular arch, discretized into 62 rigid elements, is subjected to the self-weight and to horizontal incremental action represented by forces proportional to the mass through the scale parameter λ. Right: a representation of the solution $\boldsymbol{U}^0$ corresponding to $\lambda = 0.94$ and obtained through the simplex method.

(3) formalization of the minimum problem (20) in terms of the displacement parameters;

(4) numerical solution of the problem: determination of the static multiplier and the allied global mechanism;

(5) identification of the macroblocks moving rigidly constituting the one-degree of freedom mechanism;

(6) step-by-step linear superposition upgrading of the initial geometry;

(7) evaluation of the curve describing the total potential energy evolution;

(8) identification of the maximum displacement corresponding to a local maximum of the total potential energy.

3.1. ***Circular arch.*** The example reported here regards a circular arch subjected to horizontal forces, simulating a seismic action. The only loads considered are the self-weight and the horizontal incremental action. The horizontal forces are proportional to the mass through the scale parameter λ, and act at the centroids of each block. The circular arch we considered has a springing angle $\beta = 20°$ (total angle of embrace 140°), an internal radius $r = 1.50$ m and a thickness $s = 0.40$ m. We discretize it into 62 prismatic rigid elements as shown in Figure 1 (left).

By applying the PRD method the collapse multiplier λ_c is found to belong to the interval [0.932, 0.941]. The mechanism corresponding to $\lambda = 0.94$ reached through the simplex method in 0.04 s (with an Intel Core i7-6700HQ) is depicted in Figure 1 (right): the four hinges form and the arch becomes a one-degree of freedom mechanism whose moving part involves three rigid macroblocks.

With respect to the obtained mechanism (see Figure 2, left) a linearized kinematical incremental analysis is performed. Assuming the rotation φ_3 of the block 3 as the Lagrangian parameter governing the mechanism and by fixing a constant incremental step, namely $\delta\varphi_3 = 0.0001$ rad, the geometry of the structure at the step j is obtained by upgrading the geometry of step $(j-1)$. At each step the incremental work made by the external gravitational actions is evaluated and by summing up each increment the curve describing the total potential energy (TPE) of the load is obtained (see Figure 2, right). In this figure, the maximum static displacement corresponds to the statically unstable configuration.

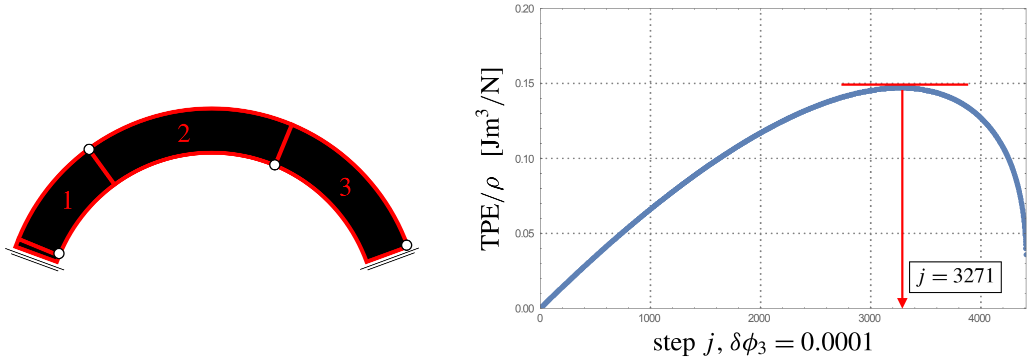

Figure 2. Partition of the arch domain obtained through the PRD method: the moving part of the structure involves 3 rigid macroblocks hinged at four points (left) and the curve describing the TPE (right), relative to the evolution of the mechanism and dimensionless with respect to the material density ρ.

The local maximum of this curve, corresponding to an unstable configuration, is reached at step 3271 for which the rotation of the block 3 is 0.3271 rad. The need of using a step-by-step superposition procedure in order to preserve the linearity has, as counterpart, the error due to small displacement fields rather than finite ones. In particular, the effect of finite displacements are reached as the summation of the effects of many small displacements controlled by a given parameter: the incremental scalar step, in this case, a constant increment $\delta\varphi_3$ of the rotation φ_3 of block 3 is assumed as a controlled parameter (e.g., Lagrangian parameter). Indeed, for small displacements, the rotation is a skew-symmetric matrix and this means that the area of a given size increases and the amount of this increment depends on the "size of the rotation". Then, to simulate finite displacements, particularly the finite rotations, a small size step can be chosen. Thus the ratio between the area in a given step and the initial area is a reasonable measure of the error committed. Definitely, the smaller is the value of the scalar controlled parameter the better is the approximation. As shown in Figure 3 (top left), the ratio between the area of each block at step j and the initial area is assumed as a measure of the error committed: the magnitude of the error is approximately of the order 10^{-5}. The rotation and the horizontal and vertical displacements of the centroid of the three moving blocks are reported in Figure 3 (top right, and bottom).

In Figure 4 four configurations of the structure are depicted: the maximum static displacement corresponding to the step $j = 3271$ is shown in Figure 4 (bottom right).

3.2. ***Simple portal under horizontal action.*** The second example regards a simple NRNT portal subjected at the top edge to a vertical uniformly distributed load q and to an external horizontal action represented by a force λQ applied at the upper left corner. Here Q is the resultant of the acting vertical loads and λ is the load scalar factor (see Figure 5, left). The NRNT portal is discretized into 528 rigid polygonal elements defining a nontrivial partition of the structural domain. Indeed, in the previous example, the arch is trivially discretized by using radial cuts and the PRD method is used only to define the location of the hinges when the mechanism forms. This is why one knows in advance that the common fractures in an arch subjected to horizontal actions are represented by radial cuts.

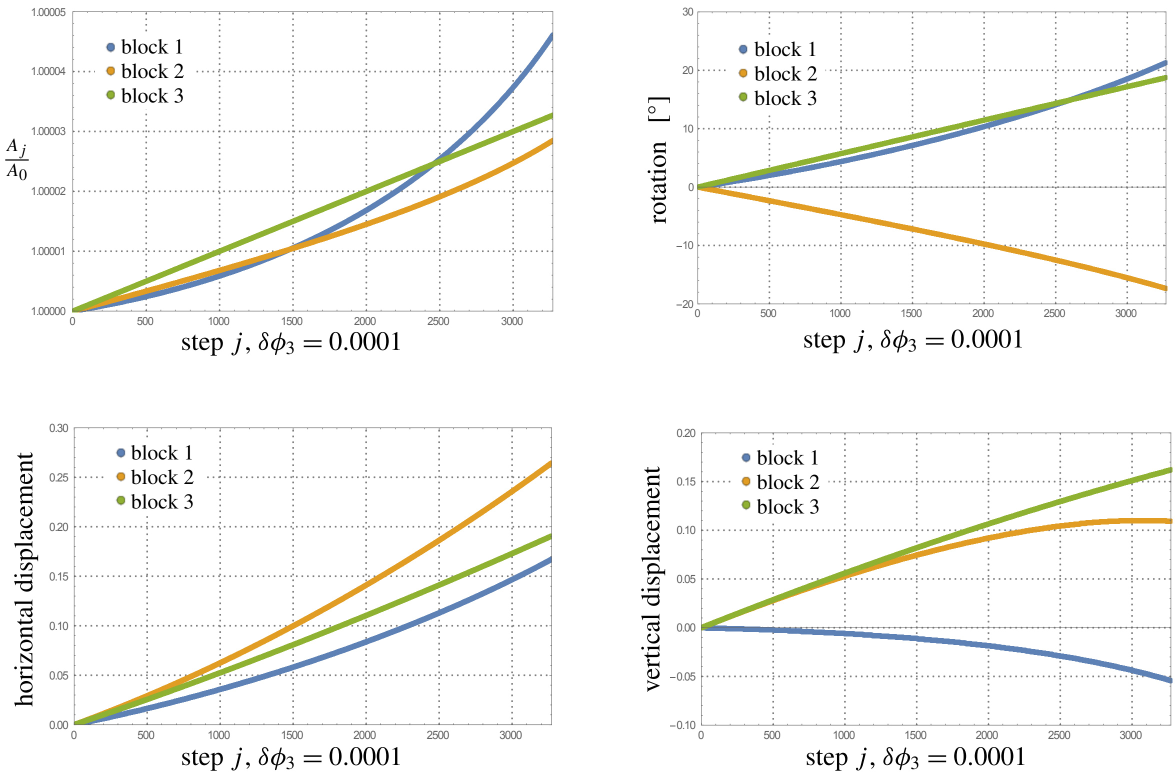

Figure 3. Top left: a measure of the error is reported by plotting the ratio between the area at the step j, namely A_j, and the initial area A_0 of each block. The number of iterations versus rotation (top right), horizontal displacement (bottom left) and vertical displacement (bottom right) of the centroid of each block.

On the contrary, in this example, it is hard to define in advance which the best discretization is: portals are characterised by vertical fractures as well as diagonal ones. One can choose to discretize this structure by using rectangular blocks, triangular blocks or another kind of discretization, but, one of the PRD method's strengths is to handle any kind of polygonal elements. With this in mind, the best way to tackle this problem is to allow for any typology of cracks, namely: vertical, horizontal and diagonal cracks. PRD method will choose the location of cracks and consequently the best rigid macroblocks partition of the domain as the one solving the minim problem (20).

Here the portal is discretised first with triangular elements, and then this discretization is further refined by allowing many other kinds of diagonal cracks for each panel. The dimension of the set of kinematical admissible mechanisms is 1584.

By applying the PRD method the collapse multiplier λ_c is found to belong to the interval [0.406, 0.412]. The mechanism corresponding to $\lambda = 0.41$ and reached through the interior point method in 0.28 s (with an Intel Core i7-6700HQ) is depicted in Figure 5 (right). In this case the structure transforms into a one-degree of freedom mechanism involving three rigid macroblocks hinged to each other at four points.

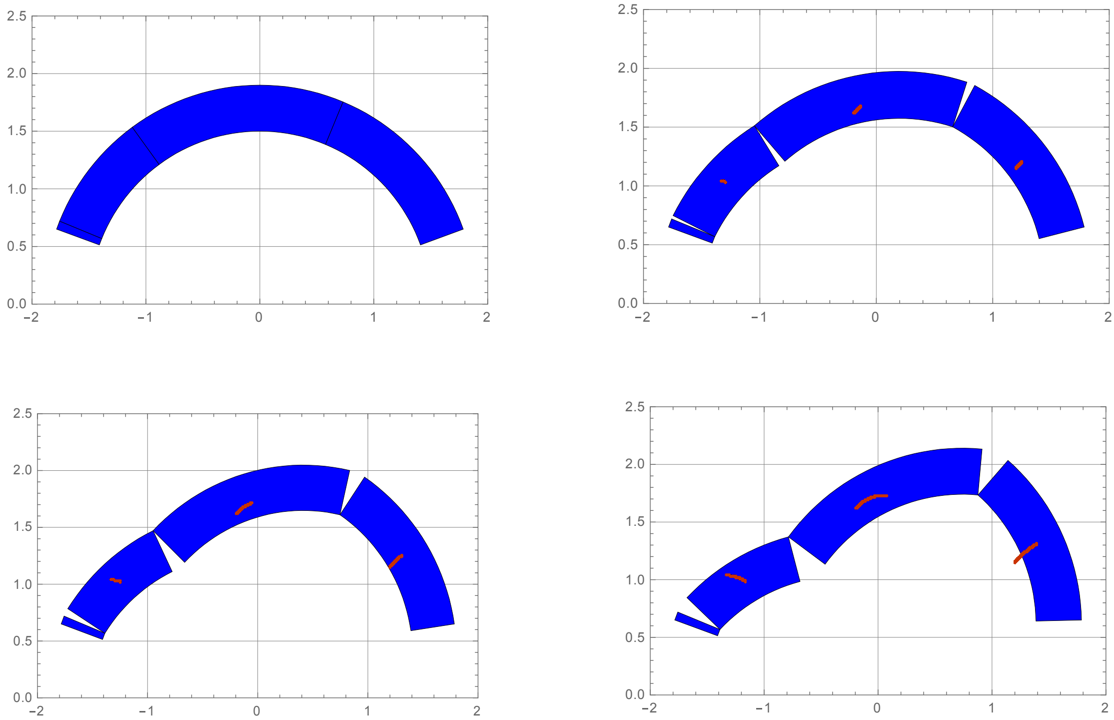

Figure 4. Configurations of the structures at four different steps: $j = 0$ (top left), $j = 1000$ (top right), $j = 2000$ (bottom left), $j = 3271$ (bottom right). The configuration at $j = 3271$ (bottom right) is unstable and represents the maximum admissible static displacement. The red line represents the paths of the centroids of each block.

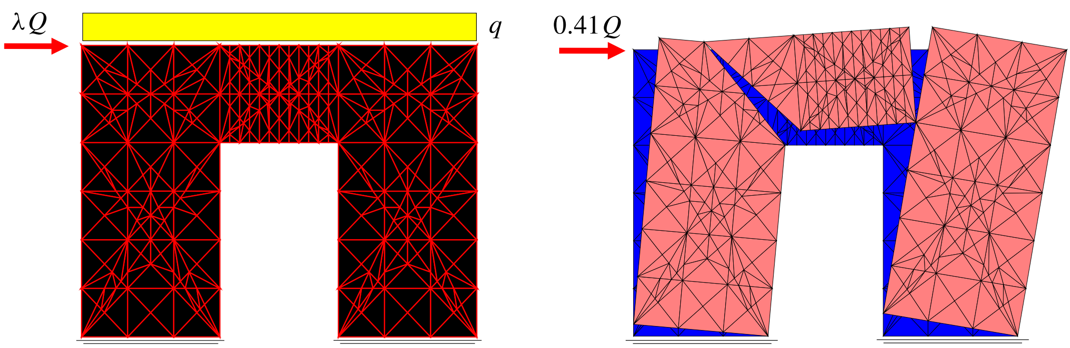

Figure 5. Left: the NRNT portal, discretized with 528 rigid polygonal elements, is subjected to a uniformly distributed load q and to the horizontal force λQ. Right: a representation of the solution $\boldsymbol{U}^0$ corresponding to $\lambda = 0.41$ and obtained through the interior point method.

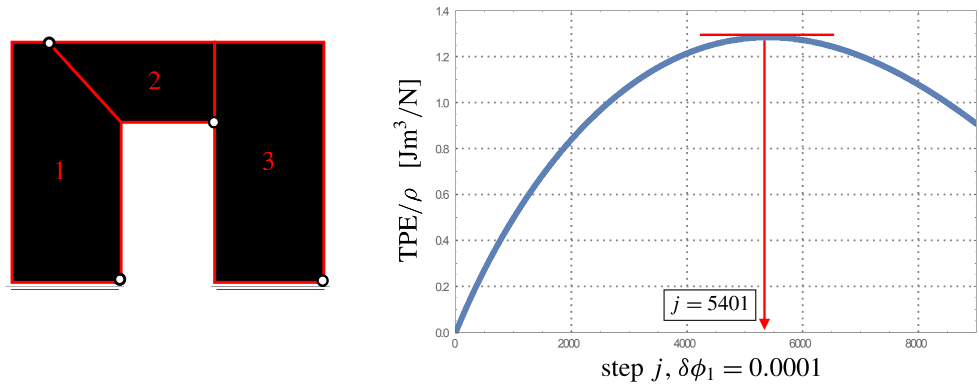

Figure 6. Left: the total potential energy (TPE), dimensionless with respect to the material density ρ, is reported: the maximum static displacement corresponds to the local maximum representing an unstable configuration. Right: a measure of the error is reported by plotting the ratio between the area at the step j and the initial area.

With respect to the mechanism shown in Figure 6 (left), a kinematical incremental analysis assuming small rigid displacements and by considering the rotation φ_1 of the block 1 as the Lagrangian parameter governing the mechanism and by fixing a constant incremental step, namely $\delta\varphi_1 = 0.0001$ rad, the geometry of the structure at step j is obtained by upgrading the geometry of step $(j-1)$ through the infinitesimal displacement field valued via the kinematical analysis. In each step the incremental work made by the external gravitational actions is evaluated. By summing each increment it is possible to obtain, as shown in previous examples, the curve describing the total potential energy of the load (see Figure 6, right).

The local maximum of this curve, corresponding to an unstable configuration, is reached at step 5401 for which the rotation of the block 1 is 0.5401 rad. In Figure 7 (left) a measure of the error committed considering small rigid displacements is reported showing the ratio between the area of each block at step j and the initial area. The rotation, the horizontal and the vertical displacement of the centroid of each block are reported in Figure 7 (top right, bottom left and right, respectively). In Figure 8 four configurations of the structure are depicted: the maximum static displacement corresponding to the step $j = 5401$ is shown in Figure 8 (bottom right).

By looking at the configuration depicted in Figure 8 (bottom right) it can be seen that the unilateral restrictions among blocks have been violated; that is, tensile forces are needed to be in equilibrium in this configuration. Indeed, to have an intuitive understanding of this phenomenon it is possible to imagine the structure as forced to lie in the configuration (see Figure 8, bottom right): just after it is left free it does not come back to the starting configuration (Figure 8, top left) but it falls down. To assess and explore this phenomenon analytically it is sufficient to evaluate the internal forces acting on the interfaces depicted in Figure 9 (right). This can be done by evaluating at each step the transpose of the kinematical matrix, namely the static matrix. In particular, once the inverse problem is solved it is possible to evaluate the axial forces acting along the interfaces during all superposition processes as shown in Figure 9 (left). As it is expected starting from the step $j = 2924$ (see Figure 8, bottom left) there is traction at the *interface 2*.

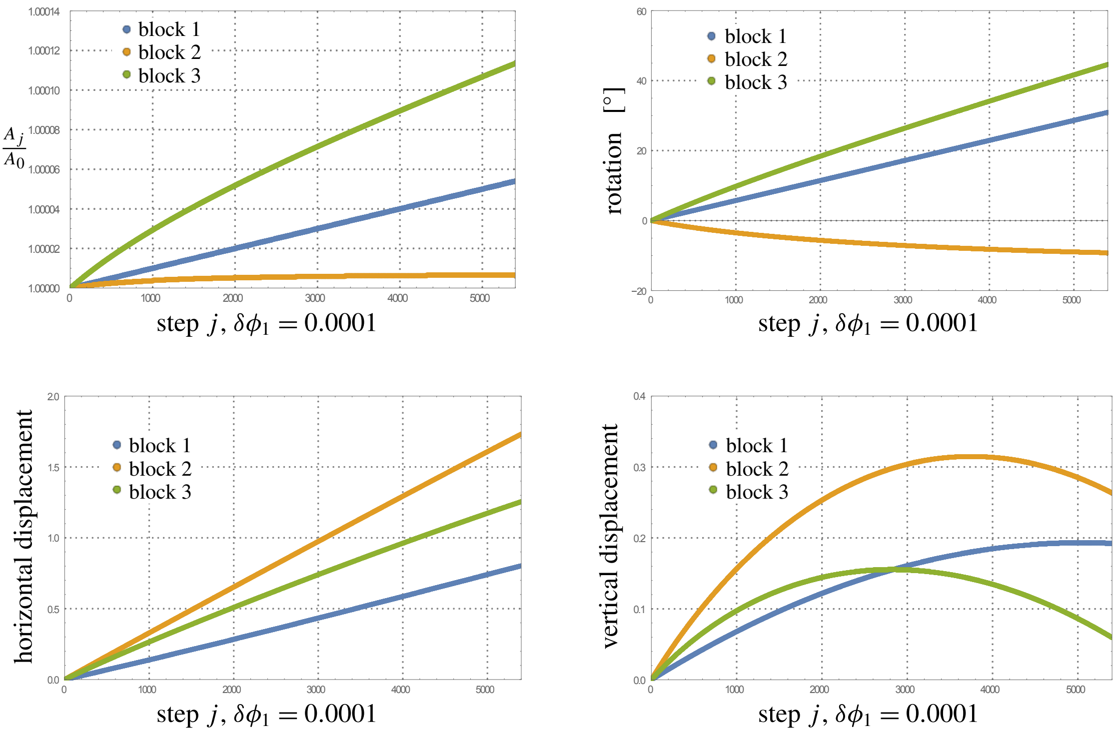

Figure 7. Top left: a measure of the error connected with the assumption of small rigid displacements is reported by plotting the ratio between the area at the step j, namely A_j, and initial area A_0 of each block. The number of iterations versus rotation (top right), horizontal displacement (bottom left) and vertical displacement (bottom right) of the centroid of each block.

4. Conclusions

In the present work, to perform a stability analysis of masonry structures under the effect of horizontal loads simulating a severe earthquake, a PRD method has been developed. The masonry has been modelled as an NRNT material on the base of Heyman's hypotheses, by which the theorems of limit analysis still hold true.

It is worth noting that the PRD mechanisms analysis arise naturally in the solution of equilibrium problem for structures made of NRNT materials. Both crack patterns and horizontal load multipliers, formulating the BVP as an energy minimum search in the space of piecewise rigid displacement, have been identified.

Due to linear contact relations between two adjacent blocks of the structural domain partition, the PRD method transforms a continuum minimum problem (11) in a linear programming one (20) in which the minimization function is the potential energy of the loads and the constraints are linearly formulated, see (21). In this context, the PRD method gives the possibility to investigate the behaviour of a generic 2D planar masonry structure subjected to settlements and load as, for example, horizontal seismic actions.

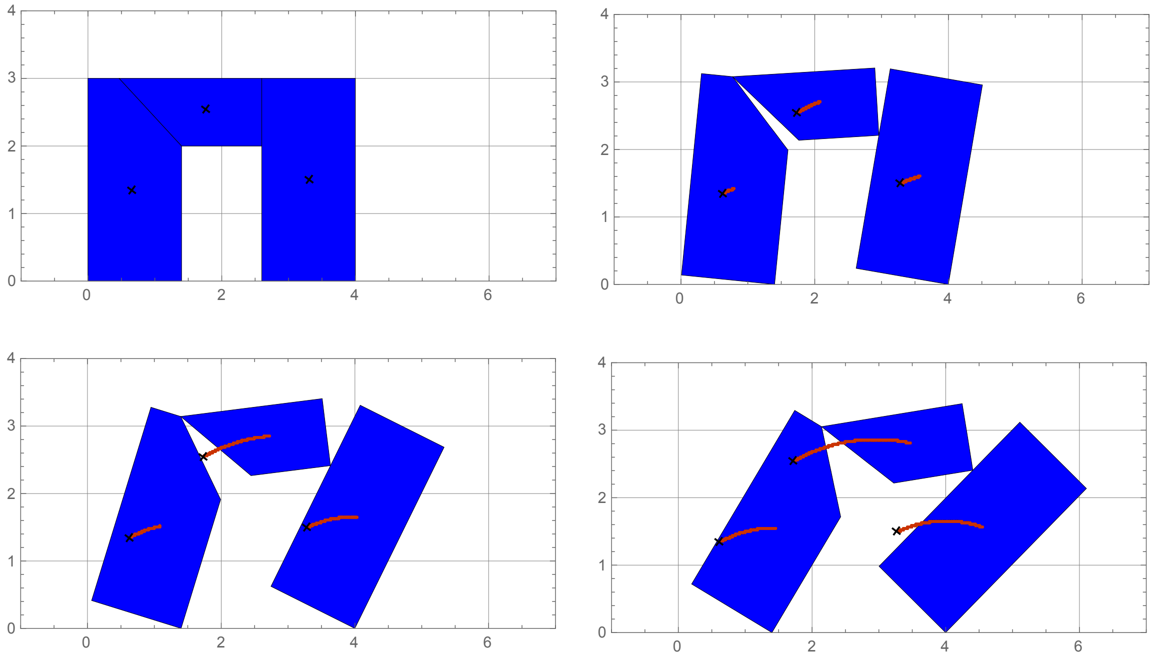

Figure 8. Configurations of the structures in different steps: $j = 0$ (top left), $j = 1000$ (top right), $j = 2924$ (bottom left), $j = 5401$ (bottom right). The configuration at $j = 5401$ (bottom right) is unstable and represents the maximum admissible static displacement. The red line represents the paths of the centroids of each block.

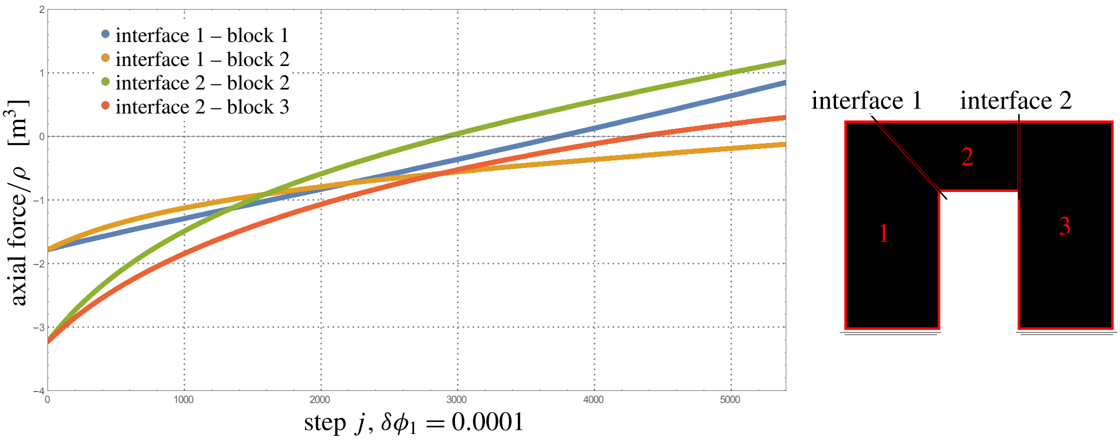

Figure 9. Axial forces (dimensionless with respect to the material density ρ) versus the number of iterations (left) acting on the interfaces (right): starting from the step $j = 2924$ the axial force acting on the interface 2 of block 2 is no longer in compression.

With PRD method both the horizontal static load multiplier and the corresponding one-degree of freedom mechanism are identified. This mechanism is employed to start a step-by-step kinematical procedure, based on small rigid displacement at each step, in order to assess the maximum horizontal displacement of the structure and to build the displacement capacity curve in finite displacement conditions. With reference to this last consideration, it is noted that the incremental PRD kinematical approach preserves the linearity of the problem and consequently it is solved in few seconds for a wide range of masonry structures.

In order to point out the potentiality of the PRD method, a circular arch and a simple portal, have been finally examined. In both cases, maximum static displacements are founded as local maximum of potential energy. As shown in the examples, a masonry structure can exhibit a large displacement before taking an unstable configuration (see [Mauro et al. 2015]).

References

[Angelillo 2014] M. Angelillo, "Practical applications of unilateral models to masonry equilibrium", pp. 109–210 in *Mechanics of masonry structures*, edited by M. Angelillo, Springer, Vienna, 2014.

[Angelillo 2015] M. Angelillo, "Static analysis of a Guastavino helical stair as a layered masonry shell", *Compos. Struct.* **119** (2015), 298–304.

[Angelillo 2019] M. Angelillo, "The model of Heyman and the statical and kinematical problems for masonry structures", *Int. J. Masonry Res. Innov.* **4**:1-2 (2019), 14–31.

[Angelillo and Fortunato 2004] M. Angelillo and A. Fortunato, "Equilibrium of masonry vaults", pp. 105–111 in *Novel approaches in civil engineering*, vol. 14, edited by M. Frémond and F. Maceri, Springer, Berlin, Heidelberg, 2004.

[Angelillo and Rosso 1995] M. Angelillo and F. Rosso, "On statically admissible stress fields for a plane masonry-like structure", *Quart. Appl. Math.* **53**:4 (1995), 731–751.

[Angelillo et al. 2005] M. Angelillo, E. Babilio, and A. Fortunato, "A numerical method for fracture of rods", pp. 277–292 in *Mechanical modelling and computational issues in civil engineering*, vol. 23, edited by M. Frémond and F. Maceri, Springer, Berlin, Heidelberg, 2005.

[Angelillo et al. 2010] M. Angelillo, L. Cardamone, and A. Fortunato, "A numerical model for masonry-like structures", *J. Mech. Mater. Struct.* **5**:4 (2010), 583–615.

[Angelillo et al. 2012] M. Angelillo, E. Babilio, and A. Fortunato, "Numerical solutions for crack growth based on the variational theory of fracture", *Comput. Mech.* **50**:3 (2012), 285–301.

[Angelillo et al. 2014] M. Angelillo, A. Fortunato, A. Montanino, and M. Lippiello, "Singular stress fields in masonry structures: Derand was right", *Meccanica* (*Milano*) **49**:5 (2014), 1243–1262.

[Angelillo et al. 2016] M. Angelillo, E. Babilio, A. Fortunato, M. Lippiello, and A. Montanino, "Analytic solutions for the stress field in static sandpiles", *Mech. Mater.* **95** (2016), 192–203.

[Angelillo et al. 2018] M. Angelillo, A. Fortunato, A. Gesualdo, I. A., and G. Zuccaro, "Rigid block models for masonry structures", *Int. J. Masonry Res. Innov.* **3**:4 (2018), 349–368.

[Block 2009] P. Block, *Thrust network analysis: exploring three-dimensional equilibrium*, Ph. D. thesis, Massachusetts Institute of Technology. Dept. of Architecture., 2009, Available at https://dspace.mit.edu/handle/1721.1/49539.

[Block and Lachauer 2013] P. Block and L. Lachauer, "Three-dimensional (3D) equilibrium analysis of gothic masonry vaults", *Int. J. Archit. Herit.* **8**:3 (2013), 312–335.

[Block et al. 2006a] P. Block, T. Ciblac, and J. Ochsendorf, "Real-time limit analysis of vaulted masonry buildings", *Comput. Struct.* **84**:29-30 (2006), 1841–1852.

[Block et al. 2006b] P. Block, M. De Jong, and J. Ochsendorf, "As hangs the flexible line: equilibrium of masonry arches", *Nexus Netw. J.* **8**:2 (2006), 13–24.

[Brandonisio et al. 2013] G. Brandonisio, G. Lucibello, E. Mele, and A. De Luca, "Damage and performance evaluation of masonry churches in the 2009 L'Aquila earthquake", *Eng. Fail. Anal.* **34** (2013), 693–714.

[Brandonisio et al. 2015] G. Brandonisio, E. Mele, and A. De Luca, "Closed form solution for predicting the horizontal capacity of masonry portal frames through limit analysis and comparison with experimental test results", *Eng. Fail. Anal.* **55** (2015), 246–270.

[Brandonisio et al. 2017] G. Brandonisio, E. Mele, and A. De Luca, "Limit analysis of masonry circular buttressed arches under horizontal loads", *Meccanica* (*Milano*) **52**:11-12 (2017), 2547–2565.

[Cennamo and Di Fiore 2013] C. Cennamo and M. Di Fiore, "Structural, seismic and geotechnical analysis of the Sant' Agostino church in L'aquila", *Rev. Ing. Constr.* **28**:1 (2013), 7–20.

[Cennamo et al. 2018] C. Cennamo, C. Cusano, A. Fortunato, and M. Angelillo, "A study on form and seismic vulnerability of the dome of San Francesco di Paola in Naples", *Ing. Sismica* **35**:1 (2018), 88–108.

[Chiozzi et al. 2017] A. Chiozzi, G. Milani, and A. Tralli, "A Genetic Algorithm NURBS-based new approach for fast kinematic limit analysis of masonry vaults", *Comput. Struct.* **182** (2017), 187–204.

[Como 1992] M. Como, "Equilibrium and collapse analysis of masonry bodies", *Meccanica* (*Milano*) **27**:3 (1992), 185–194.

[Cundall 1971] P. A. Cundall, "A computer model for simulating progressive large scale movements in blocky rock systems", in *Proceedings of the Symposium of the International Society of Rock Mechanics* (Nancy, France), 1971.

[Dantzig 1963] G. Dantzig, *Linear programming and extensions*, Princeton University Press, 1963.

[Dantzig et al. 1955] G. B. Dantzig, A. Orden, and P. Wolfe, "The generalized simplex method for minimizing a linear form under linear inequality restraints", *Pac. J. Math.* **5**:2 (1955), 183–195.

[De Serio et al. 2018] F. De Serio, M. Angelillo, A. Gesualdo, A. Iannuzzo, G. Zuccaro, and M. Pasquino, "Masonry structures made of monolithic blocks with an application to spiral stairs", *Meccanica* (*Milano*) **53**:8 (2018), 2171–2191.

[Drei et al. 2016] A. Drei, G. Milani, and G. Sincraian, "Application of DEM to historic masonries, two case-studies in Portugal and Italy: Aguas Livres Aqueduct and Arch-Tympana of a church", pp. 326–366 in *Computational modeling of masonry structures using the discrete element method*, IGI Global, 2016.

[Forgács et al. 2017] T. Forgács, V. Sarhosis, and K. Bagi, "Minimum thickness of semi-circular skewed masonry arches", *Eng. Struct.* **140** (2017), 317–336.

[Fortunato et al. 2014] A. Fortunato, F. Fraternali, and M. Angelillo, "Structural capacity of masonry walls under horizontal loads", *Ing. Sismica* **31**:1 (2014), 41–49.

[Fortunato et al. 2015] A. Fortunato, E. De Chiara, F. Fraternali, and M. Angelillo, "Advanced models for the limit analysis of masonry structures", pp. 3716–3725 in *5th International conference on computational methods in structural dynamics and earthquake engineering* (Crete Island, Greece), 2015.

[Fortunato et al. 2016] A. Fortunato, E. Babilio, M. Lippiello, A. Gesualdo, and M. Angelillo, "Limit analysis for unilateral masonry-like structures", *Open Construct. Build. Technol. J.* **10**:Suppl 2: M12 (2016), 346–362.

[Fortunato et al. 2018] A. Fortunato, F. Fabbrocino, M. Angelillo, and F. Fraternali, "Limit analysis of masonry structures with free discontinuities", *Meccanica* (*Milano*) **53**:7 (2018), 1793–1802.

[Fraddosio et al. 2019] A. Fraddosio, N. Lepore, and M. D. Piccioni, "Lower bound limit analysis of masonry vaults under general load conditions", pp. 1090–1098 in *Structural analysis of historical constructions*, edited by R. Aguilar et al., Springer, Cham, 2019.

[Gesualdo et al. 2017] A. Gesualdo, C. Cennamo, A. Fortunato, G. Frunzio, M. Monaco, and M. Angelillo, "Equilibrium formulation of masonry helical stairs", *Meccanica* (*Milano*) **52**:8 (2017), 1963–1974.

[Gesualdo et al. 2018] A. Gesualdo, A. Iannuzzo, V. Minutolo, and M. Monaco, "Rocking of freestanding objects: theoretical and experimental comparisons", *J. Theor. Appl. Mech.* (*Warsaw*) **56**:4 (2018), 977–991.

[Giaquinta and Giusti 1985] M. Giaquinta and E. Giusti, "Researches on the equilibrium of masonry structures", *Arch. Ration. Mech. Anal.* **88**:4 (1985), 359–392.

[Heyman 1966] J. Heyman, "The stone skeleton", *Int. J. Solids Struct.* **2**:2 (1966), 249–279.

[Huerta 2008] S. Huerta, "The analysis of masonry architecture: a historical approach: to the memory of professor Henry J. Cowan", *Architect. Sci. Rev.* **51**:4 (2008), 297–328.

[Iannuzzo 2017] A. Iannuzzo, *A new rigid block model for masonry structures*, Ph. D. dissertation, Department of Structures for Engineering and Architecture, Università degli Studi di Napoli Federico II, 2017, Available at http://www.fedoa.unina.it/11732/1/Iannuzzo_Antonino_29.pdf.

[Iannuzzo et al. 2018a] A. Iannuzzo, E. Angelillo, M. De Chiara, F. De Guglielmo, F. De Serio, F. Ribera, and A. Gesualdo, "Modelling the cracks produced by settlements in masonry structures", *Meccanica* (*Milano*) **53**:7 (2018), 1857–1873.

[Iannuzzo et al. 2018b] A. Iannuzzo, A. De Luca, A. Fortunato, A. Gesualdo, and M. Angelillo, "Fractures detection in masonry constructions under horizontal seismic forces", *Ing. Sismica* **35**:3 (2018), 87–103.

[Iannuzzo et al. 2018c] A. Iannuzzo, F. De Serio, A. Gesualdo, G. Zuccaro, A. Fortunato, and M. Angelillo, "Crack patterns identification in masonry structures with a C° displacement energy method", *Int. J. Masonry Res. Innov.* **3**:3 (2018), 295–323.

[Kooharian 1952] A. Kooharian, "Limit analysis of voussoir (segmental) and concrete arches", *J. Am. Concrete Ins.* **49**:24 (1952), 317–328.

[Livesley 1978] R. K. Livesley, "Limit analysis of structures formed from rigid blocks", *Int. J. Numer. Methods Eng.* **12**:12 (1978), 1853–1871.

[Mauro et al. 2015] A. Mauro, G. de Felice, and M. J. DeJong, "The relative dynamic resilience of masonry collapse mechanisms", *Eng. Struct.* **85** (2015), 182–194.

[McInerney and DeJong 2015] J. McInerney and M. J. DeJong, "Discrete element modeling of groin vault displacement capacity", *Int. J. Archit. Herit.* **9**:8 (2015), 1037–1049.

[Mehrotra 1992] S. Mehrotra, "On the implementation of a primal-dual interior point method", *SIAM J. Optim.* **2**:4 (1992), 575–601.

[Misseri et al. 2018] G. Misseri, M. J. DeJong, and L. Rovero, "Experimental and numerical investigation of the collapse of pointed masonry arches under quasi-static horizontal loading", *Eng. Struct.* **173** (2018), 180–190.

[Ochsendorf 2006] J. Ochsendorf, "The masonry arch on spreading supports", *Struct. Eng.* **84**:2 (2006), 29–34.

[Portioli and Cascini 2016] F. Portioli and L. Cascini, "Assessment of masonry structures subjected to foundation settlements using rigid block limit analysis", *Eng. Struct.* **113** (2016), 347–361.

[Portioli et al. 2014] F. Portioli, C. Casapulla, M. Gilbert, and L. Cascini, "Limit analysis of 3D masonry block structures with non-associative frictional joints using cone programming", *Comput. Struct.* **143** (2014), 108–121.

[Rossi et al. 2017] M. Rossi, C. Calvo Barentin, T. Van Mele, and P. Block, "Collapse analysis of unreinforced masonry vaults using 3D-printed scale-model testing", pp. 327–345 in *Proceedings of the 7th International Conference on Advances in Experimental Structural Engineering* (Pavia, Italy), 2017.

[Sacco 2014] E. Sacco, "Micro, multiscale and macro models for masonry structures", pp. 241–291 in *Mechanics of masonry structures*, edited by M. Angelillo, Springer, Vienna, 2014.

[Sarhosis et al. 2016] V. Sarhosis, K. Bagi, J. V. Lemos, and G. Milani (editors), *Computational modeling of masonry structures using the discrete element method*, IGI Global, 2016.

[Shin et al. 2016] H. V. Shin, C. F. Porst, E. Vouga, J. Ochsendorf, and F. Durand, "Reconciling elastic and equilibrium methods for static analysis", *ACM Trans. Graph.* **35**:2 (2016), article 13.

[Simon and Bagi 2016] J. Simon and K. Bagi, "Discrete element analysis of the minimum thickness of oval masonry domes", *Int. J. Archit. Herit.* **10**:4 (2016), 457–475.

[Tóth et al. 2009] A. R. Tóth, Z. Orbán, and K. Bagi, "Discrete element analysis of a stone masonry arch", *Mech. Res. Commun.* **36**:4 (2009), 469–480.

[Van Mele et al. 2012] T. Van Mele, J. McInerney, M. DeJong, and P. Block, "Physical and computational discrete modeling of masonry vault collapse", pp. 2252–2560 in *Proceedings of the 8th International Conference on Structural Analysis of Historical Constructions Wroclaw* (Wroclaw, Poland), 2012.

[Vanderbei 2015] R. J. Vanderbei, *Linear programming: foundations and extensions*, Springer, 2015.

[Wolfram 2003] S. Wolfram, *The Mathematica book*, fifth ed., Wolfram Media, 2003.

[Zampieri et al. 2018] P. Zampieri, F. Faleschini, M. A. Zanini, and N. Simoncello, "Collapse mechanisms of masonry arches with settled springing", *Eng. Struct.* **156** (2018), 363–374.

Received 11 Apr 2019. Revised 12 Sep 2019. Accepted 28 Sep 2019.

ANTONINO IANNUZZO: iannuzzo@arch.ethz.ch
Institute of Technology in Architecture, Block Research Group, ETH Zurich, Stefano-Franscini-Platz 1, 8093 Zurich, Switzerland

CARLO OLIVIERI: colivieri@unisa.it
Department of Civil Engineering, University of Salerno, 84084 Fisciano, Italy

ANTONIO FORTUNATO: a.fortunato@unisa.it
Department of Civil Engineering, University of Salerno, 84084 Fisciano, Italy

JOURNAL OF MECHANICS OF MATERIALS AND STRUCTURES

msp.org/jomms

Founded by Charles R. Steele and Marie-Louise Steele

Cover photo: Mando Gomez, www.mandolux.com

See msp.org/jomms for submission guidelines.

JoMMS (ISSN 1559-3959) at Mathematical Sciences Publishers, 798 Evans Hall #6840, c/o University of California, Berkeley, CA 94720-3840, is published in 10 issues a year. The subscription price for 2019 is US $635/year for the electronic version, and $795/year (+$60, if shipping outside the US) for print and electronic. Subscriptions, requests for back issues, and changes of address should be sent to MSP.

JoMMS peer-review and production is managed by EditFlow® from Mathematical Sciences Publishers.

PUBLISHED BY

mathematical sciences publishers

nonprofit scientific publishing

http://msp.org/

Journal of Mechanics of Materials and Structures

Volume 14, No. 5 December 2019